Interpretation of the Experimental Data on the Reduction Reaction of NO by CO on Rhodium by Monte Carlo Simulations and by Solving the Kinetic Equations of the Reaction Mechanism

Joaquín Cortés* and Eliana Valencia

Facultad de Ciencias Físicas y Matemáticas, Universidad de Chile, Casilla 2777, Santiago, Chile

Received: May 31, 2005; In Final Form: March 2, 2006

Some mechanisms of the reduction reaction of NO by CO on rhodium are analyzed and discussed, solving the kinetics equations and using Monte Carlo simulations, in terms of its ability to interpret the recent experiments of Zaera et al., who used a molecular beam method to study experimentally the kinetics of the reaction. Critical use is also made of the information on rate constants available for this system in the literature. Uniform catalytic surfaces and the statistical incipient percolation cluster (IPC) fractal are considered in the simulations.

Introduction

The catalytic reduction of NO by CO (CO−NO reaction) on noble metals, especially rhodium supported on silica and alumina, has been studied extensively over the last 20 years because of its importance in catalytic converters used to control NO_x emission from mobile sources such as automotive exhaust gases.[1] This reaction has also been one of the classical prototype surface reactions which under flow conditions are good examples of nonequilibrium systems that show interesting behaviors such as dissipative structures, oscillations, kinetics phase transitions, and so forth, as has been very well reviewed by Evans,[2] Zhdanov,[3] and Albano.[4] These aspects have been of great interest to our research group for several years, both in our experimental work[5] and in the lines in which we use Monte Carlo (MC) simulations[6] and theoretical developments[7] to study basic aspects of the dynamics of irreversible systems.

In this paper, we would like to consider some recent developments related to a series of molecular beam studies carried out by Zaera and co-workers[8] at the University of California on the CO−NO reaction on rhodium, which apparently reveals the formation of the (NNO)* intermediate as a requirement for the production of molecular nitrogen, in addition to the formation of N-islands on the surface. Under these assumptions, Zaera, in collaboration with the group of Zgrablich, have carried out MC studies[9,10] assuming a new mechanism for the CO−NO reaction that considers the existence of the (NNO)* intermediate and excludes the recombination of adsorbed nitrogen as the main compound responsible for the production of molecular nitrogen, as had been proposed frequently in previous kinetics mechanisms.

Considering the interest derived from the new situation in the controversial history of the mechanism of the CO−NO reaction, in this paper, we would like to discuss some aspects, consequences, and possibilities of the mechanism taking into account the new experiments, particularly in relation to possible magnitudes of the experimental rate constants, in contrast with the above-mentioned model studied by MC in which arbitrary constants have been assumed, allowing only a qualitative view of the system's behavior which could also be far from reality in the laboratory. By solving kinetics equations and using MC simulations, the behavior of the mechanisms on a uniform catalyst and on the statistical incipient percolation cluster (IPC) fractal will be studied.

Reaction Mechanism. Over the years, a series of mechanisms have been proposed for the CO−NO reaction in a history that has not lacked arguments, particularly in relation to the production of N_2 and N_2O which, together with CO_2, are the typical products seen in this reaction. Among the most representative work in this relation, the following old papers by Hecker and Bell,[11] Oh et al.,[12] and later those of Cho[13] should be mentioned. Then, as a result of experimental work with rhodium, Permana et al.[14] and Peden et al.[15] proposed a Langmuir−Hinshelwood (LH) type mechanism for this reaction that has been largely accepted in current literature and which we have called mechanism 1 in Table 1, where CO(a), NO(a), N(a), and O(a) are the species on the surface. Recently, Chuang and Tan[16] have suggested a new mechanism that takes into account the existence of the positively or negatively charged NO species $Rh-NO^+$ and $Rh-NO^-$ on the surface, which would describe the behavior of the CO−NO reaction on supported Rh catalysts. Research on this mechanism is very recent, however, and the values of its kinetic constants are still unknown.

In a joint paper, Zaera and Zgrablich et al.[10] have considered a model that will be of special interest in this work, in which two steps of mechanism 1 are replaced by the formation, desorption, and decomposition of an intermediate species (NNO)*. Table 1 also shows this model, which we have called mechanism 2. The authors also include an Eley−Rideal (ER) type step for the formation of the intermediate that will not be considered in this paper.

With the proposed mechanism, Zaera and Zgrablich carried out an MC study of the system's behavior assuming arbitrary rate constants for the elementary steps. In the literature, however, various mechanisms have been published which include steps that may be homologized with those proposed in mechanism 2 and whose kinetic constants have been determined in the laboratory under various experimental conditions. For example, Granger et al.[17] studied the CO−NO reaction on Pt and Rh considering a mechanism similar to that of mechanism 1, including additionally the production of delta nitrogen as a result

* To whom correspondence should be addressed. E-mail: jcortes@dqb.uchile.cl.

10.1021/jp052885c CCC: $30.25
Published on Web 03/30/2006

TABLE 1: Mechanisms of the CO−NO Reaction Used in the Paper

Mechanism 1

$CO + S \xleftrightarrow[k_2]{k_1} CO_{(a)}$	$CO_{(a)} + O_{(a)} \xrightarrow{k_6} CO_2 + 2S$
$NO + S \xleftrightarrow[k_4]{k_3} NO_{(a)}$	$2N_{(a)} \xrightarrow{k_7} N_2 + 2S$
$NO_{(a)} + S \xrightarrow{k_5} N_{(a)} + O_{(a)}$	$NO_{(a)} + N_{(a)} \xrightarrow{k_8} N_2O + 2S$

Mechanism 2

$CO + S \xleftrightarrow[k_2]{k_1} CO_{(a)}$	$CO_{(a)} + O_{(a)} \xrightarrow{k_6} CO_2 + 2S$
$NO + S \xleftrightarrow[k_4]{k_3} NO_{(a)}$	$N_{(a)} + NO_{(a)} \xrightarrow{k_9} (NNO)^* + S$
$NO_{(a)} + S \xrightarrow{k_5} N_{(a)} + O_{(a)}$	$(NNO)^* \xrightarrow{k_{10}} N_2O + S$
	$(NNO)^* \xrightarrow{k_{11}} N_2 + O_{(a)}$

Mechanism 3

$CO + S \xleftrightarrow[k_2]{k_1} CO_{(a)}$	$CO_{(a)} + O_{(a)} \xrightarrow{k_6} CO_2 + 2S$
$NO + S \xleftrightarrow[k_4]{k_3} NO_{(a)}$	$NO_{(a)} + N_{(a)} \xrightarrow{k_8} N_2O + 2S$
$NO_{(a)} + S \xrightarrow{k_5} N_{(a)} + O_{(a)}$	$NO_{(a)} + N_{(a)} \xrightarrow{k_{12}} N_2 + O_{(a)} + S$

of the reaction of NO(a) and N(a) on the surface. This step, which had been considered previously by Oh et al.[12] based on studies of TPD[18] and which identifies two different pathways for the formation of N_2, has been objected in later papers published by Permana et al.[14] and Peden et al.[15] The formation of delta nitrogen is also included in some mechanisms proposed for the reduction of N_2O by CO ($CO-N_2O$ reaction).[19−23]

The above considerations have led us to analyze the steps that we have called mechanism 3 in Table 1 for the CO−NO reaction. This mechanism is a consequence of the exclusion of the beta nitrogen step, as a result of which the N_2 and the N_2O must be produced between the NO(a) and the N(a) on the surface through step 8 for N_2O and that of delta nitrogen for that of N_2. In this paper, it is shown that this hypothesis interprets reasonably the experimental production data of Permana[14] and predicts the superficial nitrogen of the experiments of Zaera et al.[8]

Results and Discussion

Analysis of the Experimental Kinetic Constants. The main objective of this work is to analyze the results of a kinetic model for the CO−NO reaction that uses rate constants whose magnitudes are of the order of those obtained in laboratory experiments and in which the model is qualitatively in agreement with the recent experiments of Zaera et al.[8] on rhodium. In these experiments, it was found that when an ^{14}N-covered Rh(111) surface is exposed to $^{15}NO + CO$ beams, the molecular nitrogen produced always contains at least one ^{15}N atom. These results indicate that the molecules of ^{15}NO are always involved in the formation of molecular nitrogen, thereby excluding the beta (k_7) nitrogen step proposed in mechanism 1 of Table 1.

Even though mechanism 2 proposed by Zaera and Zgrablich[9,10] is qualitatively in agreement with these results, there is no experimental evidence of the (NNO)* intermediate and neither are its formation and desorption constants known. In this paper, we will analyze the results obtained with mechanisms 2 and 3, discussing several experimental values from the literature for their elementary steps.

The results obtained for the phase and production diagrams of the cases that will be detailed were determined for each mechanism from the analytic solution of the model's kinetic equations under the assumption of a quasi-equilibrium regime for the adsorption−desorption steps of CO and NO in the range of kinetic constants that will be used. This is a good approximation in these cases, as we showed in a recent paper[24] for mechanism 1 of Peden−Permana, where the results obtained under these assumptions were identical to the time-independent steady-state values of the coverage θ_i of the adsorbed species, determined by integration of the differential equations for the conservation of the θ_i species. In Appendix A, we have developed the main aspects of the analytic solution of the kinetic equations and the expressions for the coverages and productions used in the paper.

Table 2 gives the experimental values of the rate constants k_i used in this paper, with the corresponding references. Given constants k_1-k_4 and k_6 of Table 2, we have fitted constant k_5 with mechanism 3 to the experimental results published by Permana et al.[14] for the CO−NO reaction on Rh(111) at 623 K and at CO and NO pressures in the gas phase, P_{NO} and P_{CO}, equal to 8 Torr, with the purpose of keeping a link between our analyses and the order of magnitude of the laboratory experiment. Since in the literature there are no values for k_9, the constant for the formation of (NNO)* in mechanism 2, we have considered its value to be infinite (instant production of (NNO)* in the MC simulations and sufficiently high values in the solution of the kinetic equations).

With respect to the constants of the last two steps of mechanisms 2 and 3, two extreme values have been published

TABLE 2: Kinetics Parameters from Rh(111) Used in the Paper

event	activation energy E_i (kcal/mol)	frequency factor ν_i (s^{-1})	refs
CO desorption (k_2)	$31.6 - 4.5\theta_{CO} - 10\theta_N$	1.6×10^{14}	12
NO desorption (k_4)	29.7	4.6×10^{14}	25
NO dissociation (k_5)	$17.5 + 2\theta_{NO}$	$3.3^a(2.1) \times 10^{10}$	25
CO_2 production (k_6)	14.3	10^{12}	12
N_2 beta production (k_7)	$32.6-9\theta_N-3\theta_O$	4×10^{12}	12
N_2O dissociation (k_{11}, k_{12})-I	17.5	6.5×10^{13}	20
N_2 delta production (k_{11}, k_{12})-II	21.0	2×10^9	12

[a] Optimum value obtained with the experimental data of the reference for $T = 623$ K, $P_{CO} = P_{NO} = 8$ Torr.

in the literature that can be associated with those steps and we have analyzed these values in this study. One of them is a high value of the rate constant, which we have called (k_{11},k_{12})-I in Table 2, which corresponds to the dissociation step of N_2O determined by Belton et al.[20] in his experiments on the (CO−N_2O) reaction. This case would mean homologizing the intermediate species (NNO)* of mechanism 2 with the adsorbed particle N_2O(a). Using the same value in mechanism 3 for k_{12} would involve the assumption, however, that the dissociation of the adsorbed N_2O and the reaction between N(a) and NO(a) lead to the same intermediate chemisorbed species, an assumption that is not obvious in this case. This situation is illustrated in Figure 2 for mechanism 3 and in Figure 7c for mechanism 2, results that contradict the experiment, as will be seen below. These results and the analysis of Figure 4a show the convenience of using a small value for the kinetic constant, such as that corresponding to the production step of delta nitrogen, which we have called (k_{11},k_{12})-II in Table 2 and which has been used in the literature by Oh et al.[12] and by Granger et al.[17] in studies of the CO−NO reaction. The (k_{11},k_{12})-II constant has been used especially in this paper, allowing a reasonable interpretation of the experiments with mechanism 3.

Constant k_8, on the other hand, is determined from constant k_{12} by means of

$$r_{N_2}/r_{N_2O} = k_{12}/k_8 \tag{1}$$

which was obtained directly from the expressions for the production of N_2 and N_2O in mechanism 3.

Granger[17] considers in one of his papers for the CO−NO reaction over Rh a mechanism the same as mechanism 1 of Table 1, adding step 12 of mechanism 3, for which, applying the quasi-steady-state approximation to N adsorbed species, he gets the equation

$$\frac{4r_{N_2}}{r_{N_2}O} + 1 = \frac{k_{12} + k_8}{k_8}\sqrt{1 + \frac{8k_7k_5}{(k_{12} + k_8)^2\lambda_{NO}P_{NO}}} + \frac{3k_{12}}{k_8} \tag{1a}$$

This expression is identical to eq 1 above if the $8k_7k_5/((k_{12} + k_8)^2\lambda_{NO}P_{NO})$ ratio is very small, which happens if k_7 and k_5 are small compared to k_{12} and k_8 or the equilibrium constant for the adsorption of NO on Rh (λ_{NO}) is high, consistent with a low adsorbed nitrogen value compared to NO. In the case of mechanism 3, it does not require a high λ_{NO} since the expression is small because the beta nitrogen step ($k_7 \rightarrow 0$) either does not exist or is negligible, so the formation of nitrogen isles that takes place using mechanism 3, as will be shown below, is coherent regardless also of the competition between the expected adsorption of NO and CO in favor of NO on Rh according to Granger.[17]

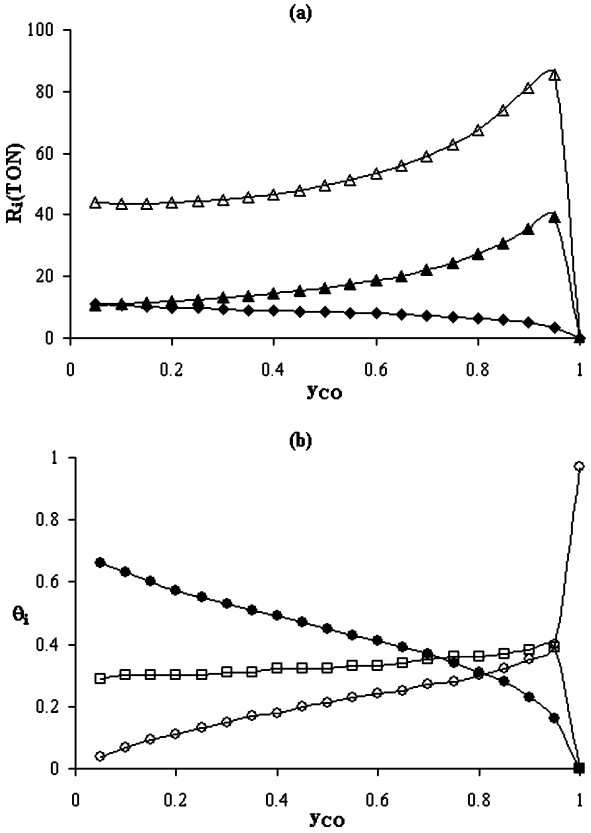

Figure 1. (a) Production (R_i,y_{CO}) and (b) phase diagram (θ_i,y_{CO}) in the steady state for mechanism 1 and the constants given in the text and in Table 2 at 623 K: (○) θ_{CO}; (●) θ_{NO}; (□) θ_N; (■) θ_O; (△) r_{CO_2}; (◆) r_{N_2}; (▲) r_{N_2O}. The lines have been drawn to guide the eyes.

Equation 1 makes it possible to use the data of Permana et al.[14] at 623 K for the selectivity, S_{N_2O}, defined by

$$S_{N_2O} = r_{N_2O}/(r_{N_2} + r_{N_2O}) \tag{2}$$

determining k_8 as a function of k_{12}, in the two cases in which we are interested, from

$$k_8 = k_{12}S_{N_2O}/(1 - S_{N_2O}) \tag{3}$$

Expressions similar to the above relate constants k_{10} and k_{11} in mechanism 2.

Results of the Solution of the Kinetic Equations. The phase and production diagrams shown in the paper extend to the whole range of CO concentrations in the gas phase, $y_{CO} = p_{CO}/(p_{CO} + p_{NO})$, assuming a total pressure equal to 16 Torr. Even though there is always some degree of arbitrariness in the assumptions made, what we have attempted to do is to observe the behavior of the new reaction mechanisms using values for the kinetic and selectivity constants of the same order of magnitude as those found in the laboratory experiment. This is different from the choice of arbitrary constants, which is typical of the line of theoretical work often published in physics journals, including some by our own group,[2−4,25] even though their objectives may be somewhat different.

In the first place, in Figure 1, we will illustrate the phase and production diagrams of the CO−NO reaction assuming the model of Peden−Permana described by mechanism 1, considering the k_i constants of Table 2, including constant k_8 suggested by Belton et al.[25] for this mechanism ($\nu_8 = 5.3 \times 10^{13}$ s^{-1}, $E_8 = 34.1$ kcal mol^{-1}). These results do not interpret the production kinetics data obtained by Permana[14] in his experiments at 623

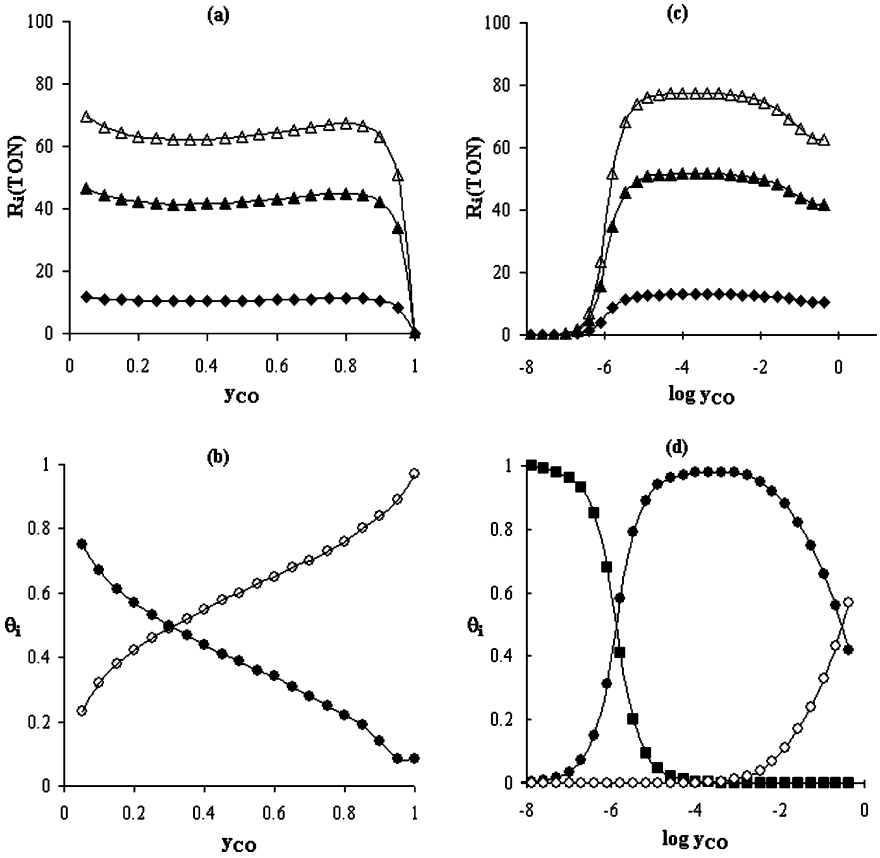

Figure 2. (a and b) Same as Figure 1 but for mechanism 3, with k_{12} corresponding to case I given in the text. (c and d) The same as parts a and b in the region of low concentrations of y_{CO}. The lines have been drawn to guide the eyes.

K for the CO−NO reaction on rhodium. On the other hand, the mechanism considers the beta nitrogen production step (k_7), contradicting the experiments of Zaera et al.[8] with labeled nitrogen atoms.

Since mechanism 1 does not allow for the interpretation of the experimental information, let us explore the possibilities of mechanism 3 for studying the problem. Figure 2 shows the phase and production diagrams of the CO−NO reaction obtained from the analytic solution of the kinetic equations of mechanism 3 in case I, where k_{12} is assumed to be equal to the dissociation constant of N_2O, and Figure 3 in case II, where k_{12} is considered equal to the production constant of delta nitrogen. The results for the first case, corresponding to high values of k_{12}, coincide exactly with those obtained from MC simulations assuming a uniform surface. In the second case, the low values of k_{12} lead to differences with the MC results, an aspect that will be discussed in the next section. It is interesting to note that in the two previous cases productions with similar orders of magnitude are obtained, with a slight maximum in the case of Figure 3 for high values of y_{CO}. However, the phase diagrams in both cases are quite different.

In the case of Figure 2b, the phase diagram shows that practically the whole surface is covered with adsorbed CO and NO, with a region rich in NO(a) at low values for the concentration of CO in the gas phase and another one rich in CO(a) at high values, while the magnitudes of the rest of the adsorbed species are negligible. The very low values obtained for the vacant site fraction θ_S show that the process of the CO−NO reaction in this case takes place on a small fraction of the surface corresponding to these vacant sites, which occur in various places of the surface due to the desorption of CO(a) and NO(a). The activity of the process occurs when a molecule of NO(a) next to a vacant site dissociates, producing N(a) and O(a) and allowing the reaction to proceed.

The phase diagram of Figure 3b shows a marked difference with the previous one, since in addition to the CO(a) and NO(a) species there is a large amount of N(a) which however does not produce a large alteration in the productions. This situation, caused by the clear difference in the value of k_{12} in both cases, which will be discussed in greater detail in the next section, is of interest in relation to the experiments of Zaera et al.,[8] which point to the existence of extensive nitrogen isles on the surface that are not reflected in the results with the data of case I.

Parts c and d of Figure 2 show the phase and production diagrams corresponding to parts a and b of Figure 2 for low concentrations of CO in the gas phase, where an interesting maximum is obtained in the production values corresponding to a maximum of surface NO(a). As the concentration of y_{CO} decreases, production drops, together with an increase in O(a) until the surface becomes poisoned with oxygen and the system becomes inactive. The appearance of surface CO(a) when the magnitude of y_{CO} increases leads to a decrease in the concentration of O(a), leaving space for the adsorption of NO. Coverage by NO reaches a maximum value in the region of highest production, where O(a) practically disappears from the surface at high concentrations of y_{CO} because CO(a) increases. Parts c and d of Figure 3 show the case of low concentrations of CO with the parameters corresponding to parts a and b of Figure 3. This case is different from the previous one because even though the productions have similar values, the phase diagram shows the existence of adsorbed nitrogen that is not removed sufficiently fast from the surface due to the lower values of k_{12} and k_8 corresponding to case II. This situation will be discussed in greater detail below.

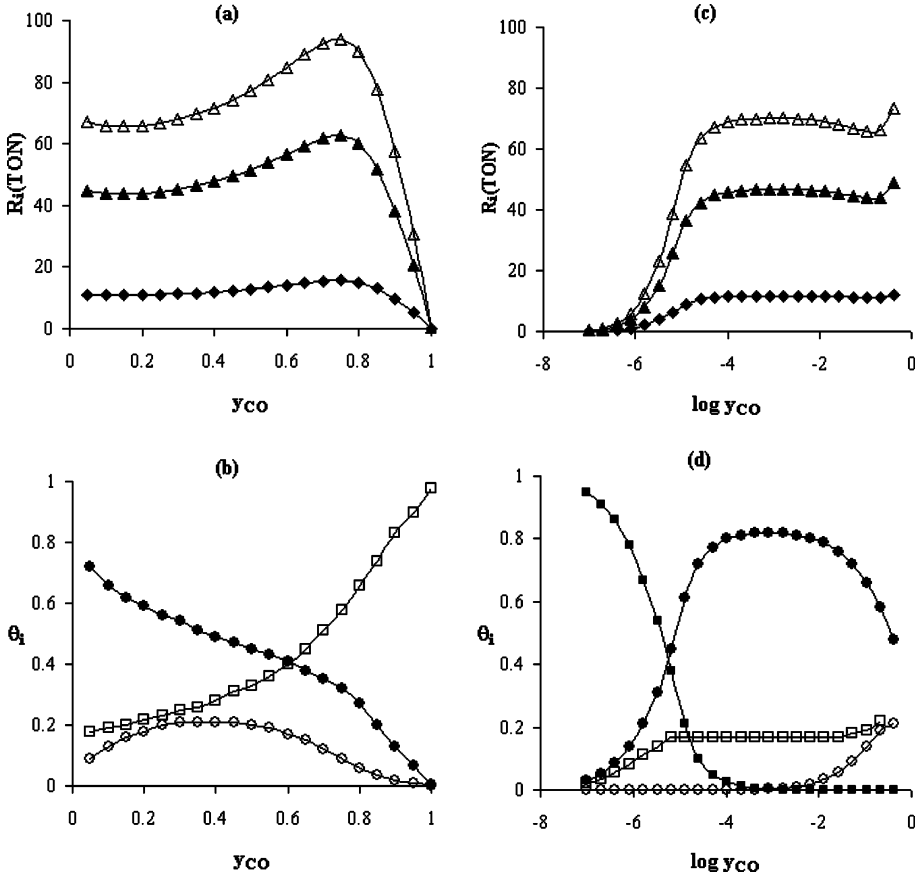

Figure 3. Same as Figure 2 with the data of case II given in the text. The lines have been drawn to guide the eyes.

Figure 4 shows the effect of changing some of the kinetic parameters in the phase and production diagrams for $y_{CO} = 0.5$. This illustrates the usefulness of getting analytic expressions for the kinetic mechanisms, allowing for an easy conceptual study of the rate constants as well as the determination of the degree of sensitivity to the results, pointing to the care that must be placed in determining the experimental values of the rate constants. The case of mechanism 3 is used as an illustration.

Parts a and b of Figure 4 show the effect of changing constant k_{12}, which has to do with the reactions between NO(a) and N(a), showing that over a wide range this constant does not have any influence on production or on the structure of the surface, indicating that the controlling step of the process is, in this case, the dissociation of NO(a). This situation is the one that corresponds to case I with high values of k_{12}. Only at low values of k_{12}, such as in the formation of delta nitrogen, which will be studied in detail in the following section, is there an important influence of this step of the mechanism, which means that if constant k_{12} continues to decrease, production will decrease and later vanish due to poisoning with N(a) that is not removed from the surface.

Parts c and d of Figure 4 show the effect of changing constant k_2, corresponding to desorption of CO, assuming the value of k_{12} of case II. An interesting effect is the maximum seen in production. It is clear that low desorption rates lead to poisoning of the surface with CO(a) without having production, while at high values, the surface is poisoned with O(a) because there is no CO(a) with which it can react, since the latter is desorbed at a high rate from the surface. Only at intermediate rates is there an adequate compensation for production to occur and that accounts for the maximum mentioned above. In this region, the existence of N(a) is also seen.

Finally, parts e and f of Figure 4 show the effect of changing k_5, the dissociation constant of NO assuming case II for the value of k_{12}. Here it is seen, for example, how the production values are strongly altered over a narrow range of the constant in the region in which the surface species CO(a) and NO(a) undergo a decrease at the expense of the appearance of adsorbed nitrogen, which at higher values of k_5 ends up poisoning the surface when the destruction steps of this substance fail to make up for its production.

Monte Carlo Simulations. Kinetics equations, like all mean field models, assume implicitly a homogeneous distribution of the adsorbed species, setting a limitation to the model and its difference with Monte Carlo simulations. However, both approximations tend to coincide if some kind of mobility of the species is established during the development of the simulations, such as an active diffusion of the adsorbed species, for example. This has not been included in this paper to retain the characteristics of the models analyzed, which do not include diffusion stages. In those cases in which there is coincidence between the mean field models and the Monte Carlo simulations, the mobility of the system's components is determined by the fast adsorption and desorption, which produces an effect similar to the diffusion of the adsorbed species.

For case I, corresponding to high values of k_{12}, the results of solving the kinetic equations and of the MC simulations, whose details are given in Appendix B, are in agreement, and in this case, the results of both mechanisms also agree. Even then, however, the MC simulations provide additional information through the snapshots. In other systems, where there is no coincidence or when the catalyst is made of a disordered surface such as the IPC, the usefulness of the simulations is clear.

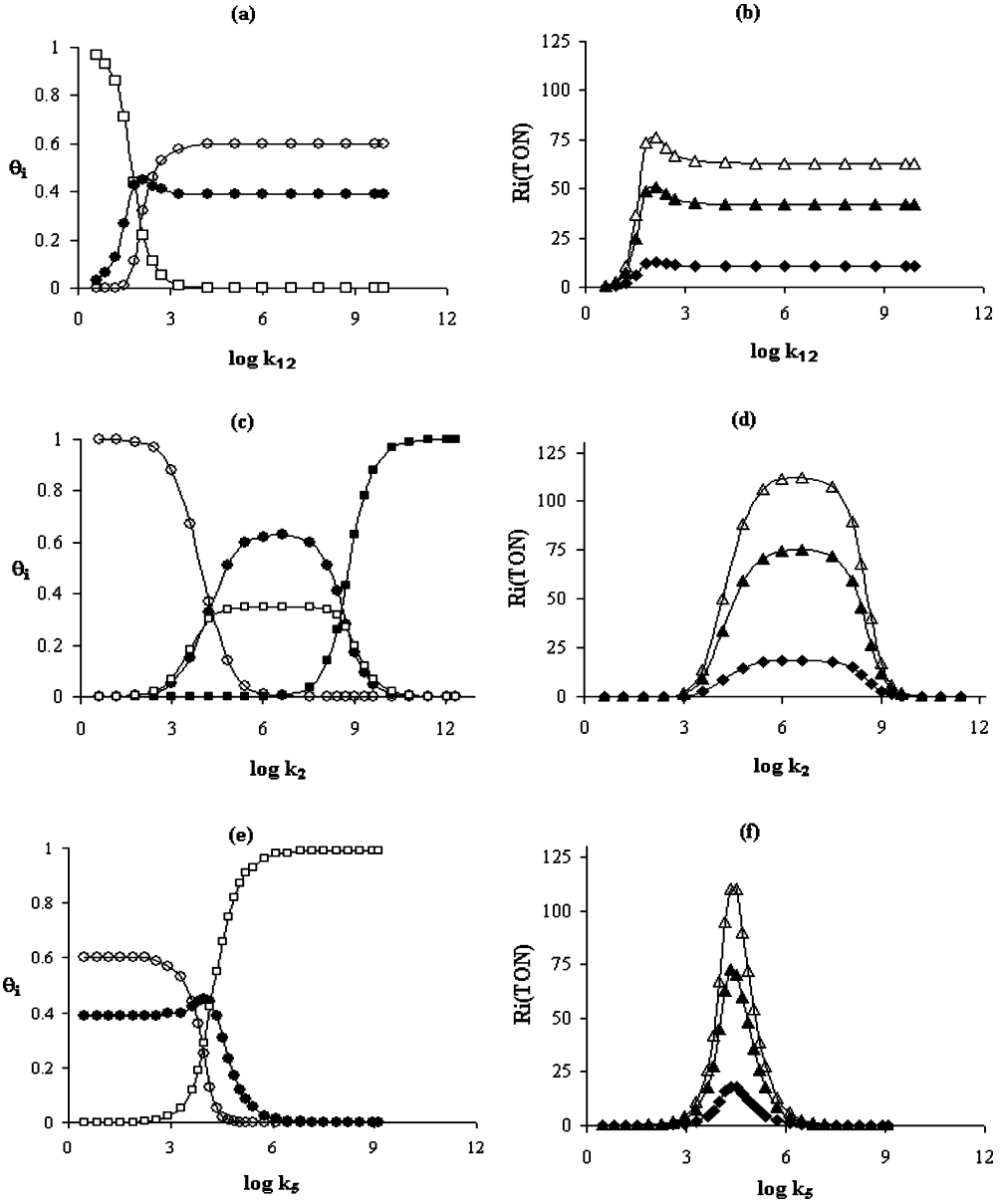

Figure 4. Productions, R_i, and concentrations, θ_i, for the changes in the various kinetics parameters for mechanism 3 at 623 K with the constants not shown equal to those of Figures 2 and 3 and $P_{CO} = P_{NO} = 8$ Torr. (a and b) Changes of constant k_{12}. (c and d) Changes of desorption constant k_2 of CO for k_{12} corresponding to case II. (e and f) Changes of dissociation constant k_5 of NO for k_{12} of case II. The lines have been drawn to guide the eyes.

The results of the phase and production diagrams of mechanism 3 on a surface assumed to be uniform are shown in parts a and b of Figure 5. They were determined by MC simulations, with data corresponding to case II for low values of constant k_{12}. Parts c and d of Figure 5 show the same case when the catalytic surface corresponds to the IPC. In this case, the simulations and the solution of the kinetic equations give different results. In this mechanism, the NO(a), supplied from the equilibrium by the NO in the gas phase, provides adsorbed nitrogen through the dissociation of NO(a) which in turn is consumed, reacting with the NO(a). It is natural, therefore, that if constants k_{12} and k_8 are high, as happens in case I for k_{12}, represented in Figure 2, then no N(a) is seen to exist on the surface because it is consumed almost completely, but it does appear when these constants are low, as in the case of Figures 3 and 5. Figure 7a represents the snapshot corresponding to mechanism 3 and case II, showing the large amount of adsorbed nitrogen that accumulates on the surface, as well as the few vacant sites distributed over the whole surface, around which the reaction occurs.

In the case of the low constants of case II and a uniform surface, there is an increase of N(a) with the increase of y_{CO}, because as NO(a) decreases, as seen in the expression of Table 2, the activation energy for the dissociation of NO(a) decreases, increasing the production rate of N(a), which is not consumed fast enough due to the low values of k_{12} and k_8. In the region of high y_{CO}, the increase of N(a) succeeds in isolating the surface O(a), which does not find CO(a) with which to react, leading to poisoning of the surface with adsorbed nitrogen and oxygen at y_{CO} greater than 75%. This does not happen with the calculation of the kinetic equations as in Figure 3, which always assumes an average situation of the surface configuration, so that there will always be some probability that the adsorbed oxygen will have some neighboring CO(a). This results in the phase diagram of Figure 3, with an ever increasing N(a) fraction and a negligible fraction of O(a) on the surface.

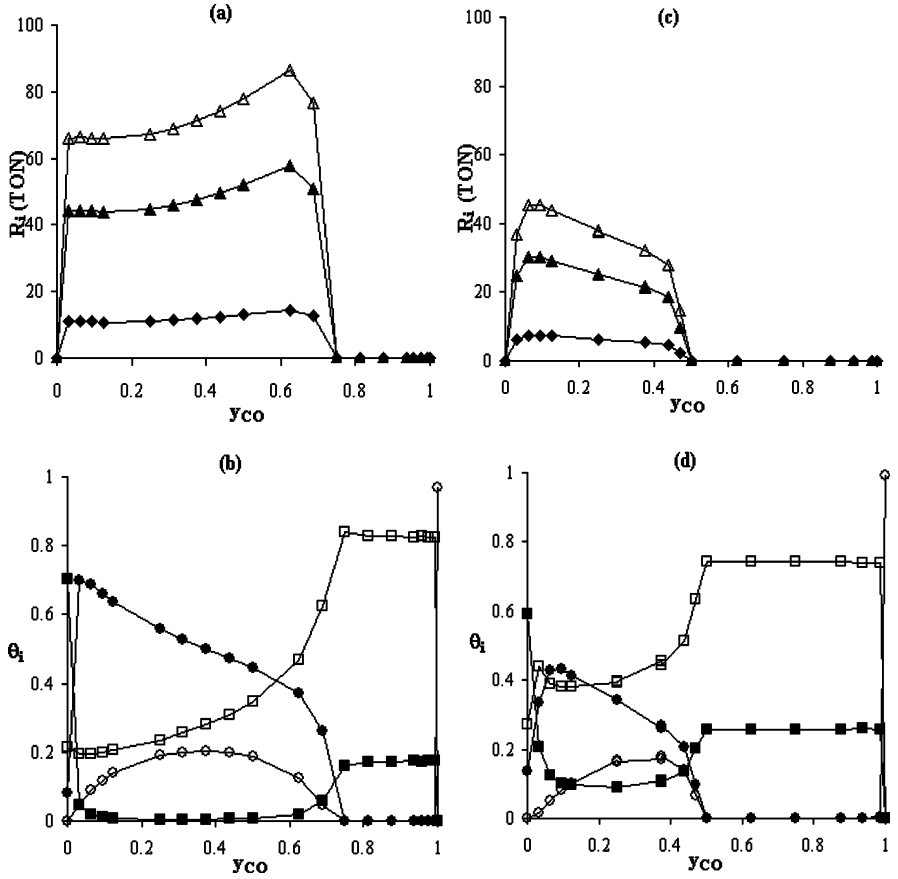

Figure 5. (a and b) Same as Figure 2 for mechanism 3, with k_{12} corresponding to case II obtained from MC simulations. (c and d) The same but on the IPC. The lines have been drawn to guide the eyes.

Parts c and d of Figure 5 show the case of the same system discussed above when the catalytic surface is the IPC fractal. Figure 7b shows the snapshot, in this case in the region poisoned with N(a) and O(a), due to the same considerations commented in the case of a uniform surface. This surface has often been used after the first papers by Albano[4] to homologize theoretically a disordered surface such as in the case of a supported catalyst. As expected, a behavior qualitatively similar to the previous one can be seen, but with a smaller production than in the case of the uniform surface, which is homologized with a crystalline catalyst, since the coordination number of the active sites is smaller, making difficult the action of those steps of the mechanism that take place between nearest neighbors (nn's) of the catalyst site. In this case, the surface poisoning is observed at lower y_{CO} values due to the lower coordination number of the surface. On the other hand, the continuous decrease of the production curves in the IPC, in contrast with the uniform case, is due to the heterogeneous distribution of neighbors around the active site in the case of this fractal.

We will now consider the behavior of the system assuming that mechanism 2 is valid, with the decomposition constant of (NNO)*, k_{11}, which is unknown, equal to the data of case II. The solution of the kinetic equations in this case gave results in agreement with those of MC for uniform surfaces. Parts a and b of Figure 6 show the phase and production diagrams on a uniform surface, and parts c and d of Figure 6 show those on the IPC.

In the first place, now one sees the existence on the surface of the intermediate species NNO*, whose superficial concentration remains approximately constant with changes of y_{CO} in the case of a uniform surface and decreases with increasing y_{CO} in the IPC. In the former case, the constant value of θ_{NNO*} can be explained because the effect of the decrease in the concentration of NO(a) on the formation of (NNO)* is made up by the increase in the production of N(a) in the dissociation step of NO(a) due to the drop of the activation energy, as shown in Table 2. In the case of the IPC, however, the formation of (NNO)*, which requires the neighborhood of N(a) and NO(a), is hindered by the lower coordination of the active site on the surface. This accounts for the continuous decrease of the production curves in the case of the IPC that is not seen on the uniform surface because, according to mechanism 2, production is proportional to the (NNO)* fraction. Figure 7c shows the snapshot obtained for this mechanism with the data of case I and a uniform surface, and the intermediate species (NNO)* is not seen in it because of the high rates of k_{10} and k_{11}, which annihilate it. It is also interesting to see the few vacant sites around which the reaction occurs, immersed between the CO(a) and NO(a) species which occupy the rest of the surface. On the other hand, Figure 7d refers to the case of the IPC and the low rate of case II for mechanism 2, showing the (NNO)* surface species and a small fraction of vacant sites.

It is important to note, finally, that no adsorbed nitrogen is seen in the case of mechanism 2, either at low or high N_2O and N_2 production rates from the intermediate (NNO)*, and at least for the conditions studied, this means that this mechanism does not allow, as happens with mechanism 3, an interpretation of the experimental results of Zaera el al.,[8] who found N(a) on the surface during the reaction.

Conclusions

Through the solution of kinetic equations and Monte Carlo simulations, the mechanisms that attempt to interpret the recent experiments of Zaera et al.[8] on the CO−NO reaction on rhodium

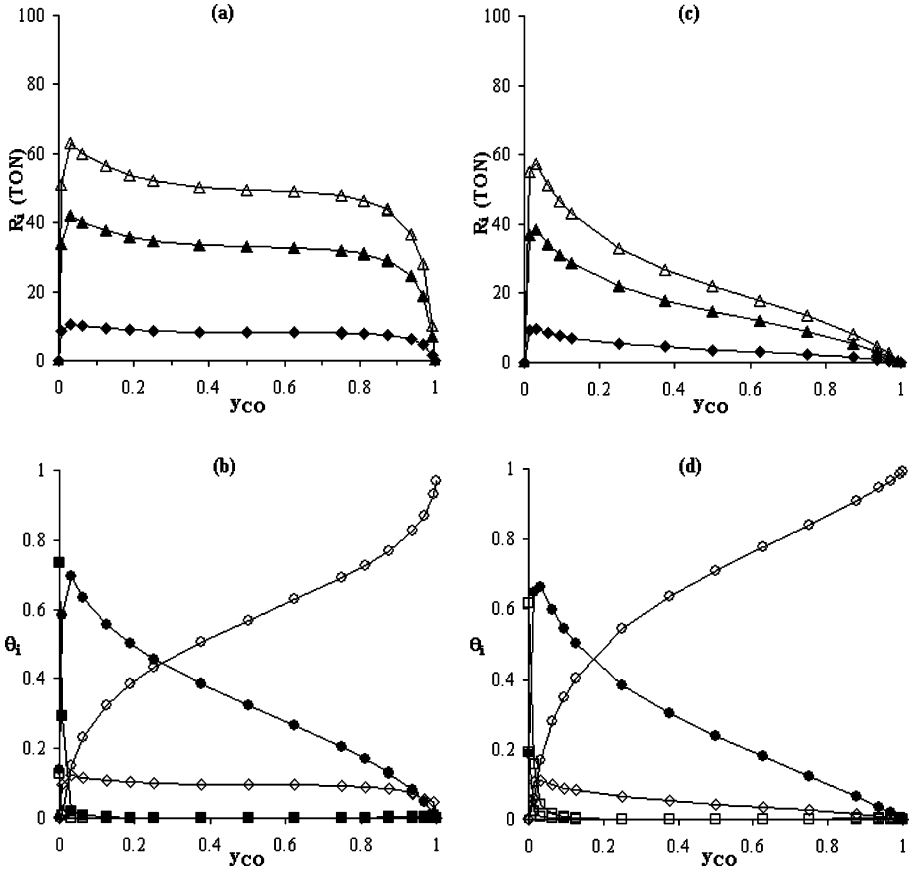

Figure 6. Same as Figure 5 for mechanism 2 and (◇) $\theta_{(NNO)^*}$. The lines have been drawn to guide the eyes.

have been discussed, considering different experimental values for the rate constants published in the literature. The study was made assuming a uniform catalytic surface and one consisting of a statistical fractal, the IPC. A sensitivity analysis was also made of the kinetic constants, and the behavior of the configuration of the surface species during the reaction was made on both uniform and disordered surfaces.

Several interesting aspects were found, particularly the fact that on a uniform surface with a mechanism that does not consider beta nitrogen, the results obtained interpret reasonably well the order of magnitude of the production as well as its constancy with pressure changes among the experimental data. This does not happen with the mechanism published earlier by Permana[14] and Peden,[15] which assumes the existence of beta nitrogen. The existence of surface nitrogen seen in the molecular beam experiments of Zaera et al.,[8] on the other hand, is interpreted adequately by a new mechanism studied in this paper (mechanism 3), which homologizes the one proposed by Bustos, Zaera, and Zgrablich et al.[9,10] (mechanism 2), if a slow rate is assumed for the production steps of N_2O and N_2, equal to the rate of production of delta nitrogen, for example. This means that a mechanism like the one proposed can interpret the experimental information published in relation to production, as well as the new experimental information of Zaera et al. referring to the composition of the adsorbed phase, if adequate experimental kinetic constants are used.

Acknowledgment. The authors acknowledge the financial support of this work by FONDECYT under Project No. 1030759.

Appendix A

Analytic Solution of the Reaction Models used in the Paper. In a manner similar to the development shown in one of our previous papers[24] for mechanism 1, we will synthesize the equations used in this paper for the other two mechanisms. Since all of them assume that the CO(a) and NO(a) adsorbates are in equilibrium with the gas phase, it is possible to write the relations

$$K_{CO} = \frac{\theta_{CO}}{\theta_S P_{CO}}$$

$$K_{NO} = \frac{\theta_{NO}}{\theta_S P_{NO}} \qquad \text{(A1)}$$

where the equilibrium constants are expressed as functions of the coverages θ_{CO} and θ_{NO}, and the partial pressures P_{CO} and P_{NO} of the gas phase, and θ_S represents the coverage of the vacant surface sites. The procedure used consists of expressing the coverages θ_i as functions of θ_{CO}, for which, if we define

$$A = \frac{P_{NO} K_{NO}}{P_{CO} K_{CO}} \qquad \text{(A2)}$$

$$B = \frac{1}{P_{CO} K_{CO}} \qquad \text{(A3)}$$

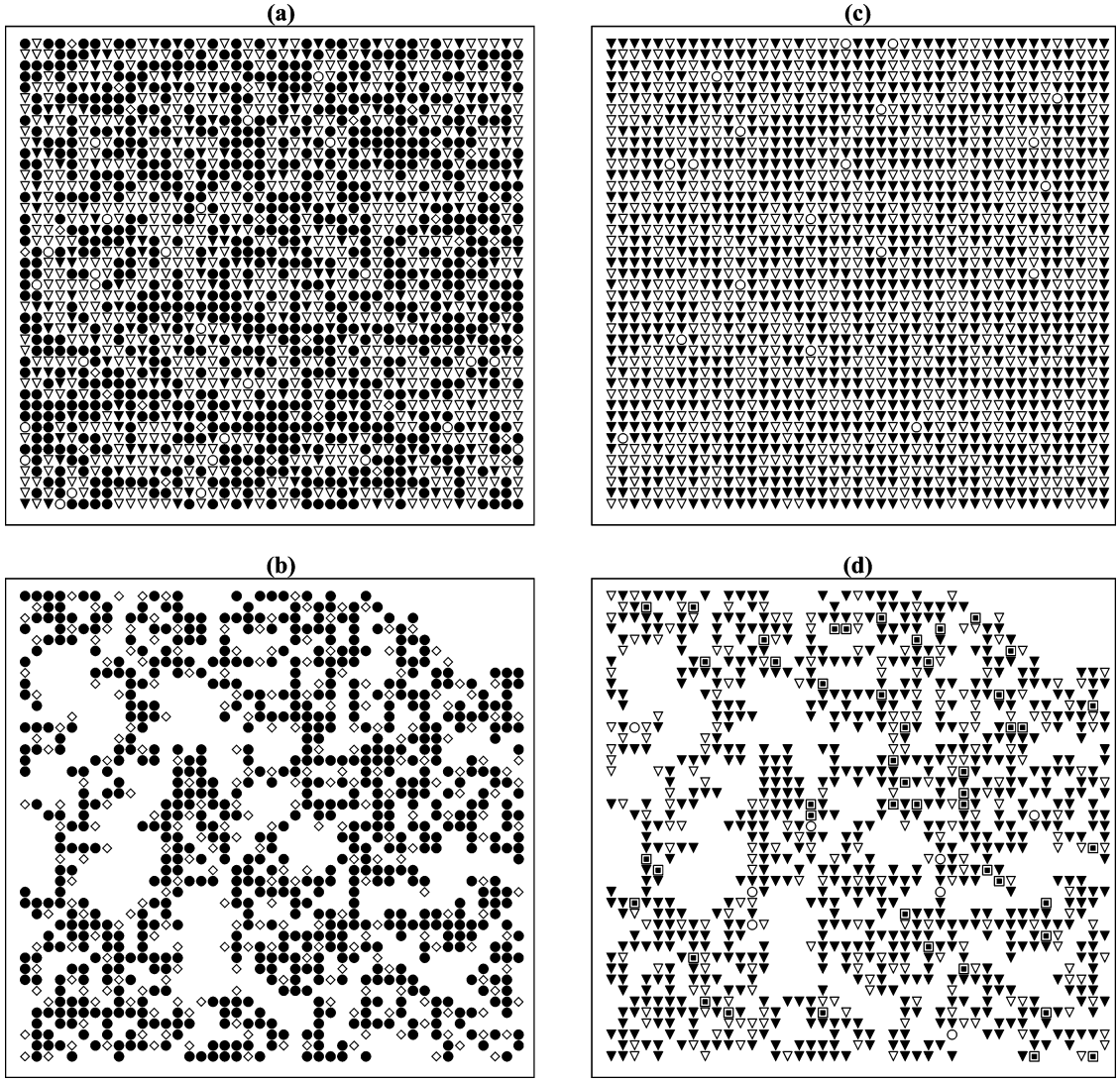

Figure 7. Snapshots of the MC simulations at 623 K corresponding to (a) mechanism 3, uniform surface, k_{12} of case II, $y_{CO} = 0.625$. (b) Mechanism 3, IPC, k_{12} of case II, $y_{CO} = 0.875$. (c) Mechanism 2, uniform surface, k_{11} of case I, $y_{CO} = 0.5$. (d) Mechanism 2, IPC, k_{11} of case II, $y_{CO} = 0.5$. (▼) = CO; (○) = vacuum; (◇) = O; (▽) = NO; (●) = N; (filled square inside open square) = (NNO)*.

it is possible to write the relations

$$\theta_{NO} = A\theta_{CO}$$

$$\theta_S = B\theta_{CO} \tag{A4}$$

Relations for Mechanism 3. In this case, it is possible to write the following conservation equations, where the first two represent the steady state for the surface species $N_{(a)}$ and $O_{(a)}$ ($d\theta_N/dt = 0$ and $d\theta_O/dt = 0$)

$$k_5\theta_{NO}\theta_S - (k_8 + k_{12})\theta_{NO}\theta_N = 0 \tag{A5}$$

$$k_5\theta_{NO}\theta_S + k_{12}\theta_{NO}\theta_N - k_6\theta_{CO}\theta_O = 0 \tag{A6}$$

$$\theta_S + \theta_{CO} + \theta_{NO} + \theta_N + \theta_O = 1 \tag{A7}$$

If we define the relations

$$C = \frac{k_5 B}{k_8 + k_{12}} \tag{A8}$$

$$D = \frac{k_5 AB + k_{12} AC}{k_6} \tag{A9}$$

it is possible to write

$$\theta_N = C\theta_{CO}$$

$$\theta_O = D\theta_{CO} \tag{A10}$$

so that from eq A7 we have

$$\theta_{CO} = 1/(1 + A + B + C + D) \tag{A11}$$

Therefore, the productions r_i are the following

$$r_{CO_2} = k_6\theta_{CO}\theta_O$$

$$r_{N_2} = k_{12}\theta_{NO}\theta_N$$

$$r_{N_2O} = k_8\theta_{NO}\theta_N \tag{A12}$$

Relations for Mechanism 2. Similarly to the previous case, we now consider the following conservation equations, the first three of which represent the steady state for the surface species

$N_{(a)}$, $O_{(a)}$, and $(NNO)^*_{(a)}$ ($d\theta_N/dt = 0$, $d\theta_O/dt = 0$, and $d\theta_{(NNO)^*}/dt = 0$)

$$k_5\theta_{NO}\theta_S - k_9\theta_{NO}\theta_N = 0 \quad \text{(A13)}$$

$$k_5\theta_{NO}\theta_S + k_{11}\theta_{(NNO)^*} - k_6\theta_{CO}\theta_O = 0 \quad \text{(A14)}$$

$$k_9\theta_{NO}\theta_N - (k_{10} + k_{11})\theta_{(NNO)^*} = 0 \quad \text{(A15)}$$

$$\theta_S + \theta_{CO} + \theta_{NO} + \theta_N + \theta_O + \theta_{(NNO)^*} = 1 \quad \text{(A16)}$$

If we define the relations

$$C' = \frac{k_5 B}{k_9} \quad \text{(A17)}$$

$$D' = \frac{k_5 AB}{k_{10} + k_{11}} \quad \text{(A18)}$$

$$E = \frac{(k_{10} + 2k_{11})D}{k_6} \quad \text{(A19)}$$

$$F = 1 + A + B + C\grave{} + E \quad \text{(A20)}$$

it is possible to write

$$\theta_N = C'\theta_{CO} \quad \theta_{(NNO)^*} = D'\theta_{CO}{}^2 \quad \text{(A21)}$$

$$\theta_O = E\theta_{CO} \quad \theta_{CO} = \frac{-F + (F^2 + 4D')^{1/2}}{2D'} \quad \text{(A22)}$$

where in eq A22 only solutions that make θ_{CO} positive have been considered. The productions r_i are the following

$$r_{CO_2} = k_6\theta_{CO}\theta_{CO}$$

$$r_{N_2} = k_{11}\theta_{(NNO)^*}$$

$$r_{N_2O} = k_{10}\theta_{(NNO)^*} \quad \text{(A23)}$$

Appendix B

Simulation Procedure. The MC algorithm used in this paper is similar to one used previously by our group[27] for the CO oxidation reaction, based on one proposed earlier for this system[28] and recently for the CO−NO reaction.[29] For the CO−NO reaction, the simulation process starts by selecting an event from the mechanism (adsorption, desorption, dissociation, or reaction) according to the probability, p_i, of the event defined by

$$p_i = k_i / \sum_i k_i \quad \text{(B1)}$$

where k_i corresponds to the rate constant of step i of the mechanism. It is assumed that the rate constants k_i can be expressed as functions of temperature T according to Arrhenius' equation

$$k_i = \nu_i \exp(-E_i/RT) \quad \text{(B2)}$$

where E_i is the activation energy and ν_i is the frequency factor. In the case of adsorption, k_i is calculated according to the expression of the kinetic theory of gases

$$k_i(\text{ads}) = S_i\sigma(2\pi M_i RT)^{-1/2} \quad \text{(B3)}$$

where M_i is the molecular mass of i, S_i is the corresponding sticking coefficient, and the coefficient σ is the area occupied by 1 mol of surface metal atoms (3.75×10^8 cm^2/mol for Rh-(111)).

The MC algorithm begins with selection of the event. If it corresponds to the adsorption of CO, a site is chosen randomly on the surface, and if it is vacant, a $CO_{(a)}$ particle will be adsorbed. If the site is occupied, the attempt is ended. If the adsorption of NO is chosen, the procedure is completely analogous and an $NO_{(a)}$ particle is adsorbed.

If CO desorption is chosen, a surface site is selected randomly. If it is occupied by a particle different from $CO_{(a)}$ or it is vacant, the attempt is ended. However, if it is occupied by a $CO_{(a)}$ particle, desorption occurs and the particle is replaced by a vacant site. The procedure is analogous in the case of choosing the desorption of NO.

When the chosen event is the dissociation of NO, a surface site is chosen randomly. If it is occupied by an $NO_{(a)}$ particle, a nearest neighbor (nn) site is chosen randomly next to the first site. If this is empty, dissociation occurs and an $N_{(a)}$ particle remains in the first site and an $O_{(a)}$ particle in the second site.

In the case of chemical reaction events that involve two reactant particles, a site on the surface is first chosen randomly. If it is occupied by a particle corresponding to one of the reactants, a nearest neighbors (nn's) site is then chosen randomly next to the first site. If the latter is occupied by the other particle of the same reaction, the event is successful and a product molecule is removed from the surface leaving two vacant sites. For example, if the first particle is $CO_{(a)}$ and the second is $O_{(a)}$, a molecule of CO_2 leaves the surface. If the reactant is particle $(NNO)^*$ and the chosen site contains this particle, one proceeds as follows: If the reaction chosen is the dissociation of $(NNO)^*$, $N_{2(g)}$ is produced and $O_{(a)}$ remains in the chosen site. But if it corresponds to the formation of $N_2O_{(g)}$, a vacant site remains.

In the case of the formation of $(NNO)^*$ in mechanism 2, which occurs at an infinite rate, the process is carried out in such a way that every time in a step the pair of nn's corresponding to $NO_{(a)}$ and $N_{(a)}$ appears, the intermediate complex $(NNO)^*$ is formed instantly at the site where $NO_{(a)}$ was, leaving a vacant site.

The substrates used in the simulations were a uniform surface made of sites located in an LxL square lattice and a statistical fractal, the incipient percolation cluster (IPC), whose active sites were generated by blocking a fraction equal to 0.407254 of the LxL sites (impurities) of the square lattice, with a fractal dimension equal to 91/48.[30] The substrates are obtained in this case by considering only the spanning cluster of the remaining sites computed by Kopelman's algorithm.[31] Since the IPC is probabilistic or nondeterministic, it was necessary to generate a number of them, so that the properties obtained from MC for the CO−NO reaction are the average of the results of the simulations carried out on those substrates.

In general, to reach an adequate stability in the results, use was made of a number of iterations of the order of 10^7 MCS (Monte Carlo steps), defined as the number of attempts equal to the number of sites in the substrate.

References and Notes

(1) Taylor, K. C. *Catal. Rev. Sci. Eng.* **1993**, *457*, 35. Shelef, M.; Graham, G. *Catal Rev. Sci. Eng.* **1994**, *36*, 433.

(2) Evans, J. W. *Langmuir* **1991**, *7*, 2514.

(3) Zhadanov, V. P.; Kasemo, B. *Surf. Sci. Rep.* **1994**, *20*, 111.

(4) Albano, E. V. *Heterog. Chem. Rev.* **1996**, *3*, 389. Albano E. V.; Borowko, M. *Computational Methods in Surface and Colloid Science*; Marcel Dekker: New York, 2000; Chapter 8, pp 387−437.

(5) Araya, P.; Gracia, F.; Cortes, J.; Wolf, E. E. *Appl. Catal. B* **2002**, *38*, 77.

(6) Cortes, J.; Puschmann, H.; Valencia, E. *J. Chem. Phys.* **1997**, *106*, 1467. Cortes, J.; Valencia, E. *Phys. Rev. E* **2003**, *68* (1), 016111. Cortes, J.; Valencia, E. *J. Phys. Chem. B* **2004**, *108* (9), 2979−2986.

(7) Cortes, J.; Puschmann, H.; Valencia, E. *J. Chem. Phys.* **1998**, *109*, 6086. Cortes, J.; Valencia, E.; Puschmann, H. *Phys. Chem. Chem. Phys.* **1999**, *1*, 1577. Cortes, J.; Narvaez, A.; Puschmann, H.; Valencia, E. *Chem. Phys.* **2003**, *288*, 77.

(8) Zaera, F.; Gopinath, Ch. S. *J. Chem. Phys.* **1999**, *111*, 8088. Zaera, F.; Gopinath, Ch. S. *Chem. Phys. Lett.* **2000**, *332*, 209. Zaera, F.; Gopinath, Ch. S. *J. Chem. Phys.* **2002**, *116*, 1128.

(9) Bustos, V.; Gopinath, Ch. S.; Unac, R.; Zaera, F.; Zgrablich, G. *J. Chem. Phys.* **2001**, *114*, 10927.

(10) Bustos, V.; Unac, R.; Zaera, F.; Zgrablich, G. *J. Chem. Phys.* **2003**, *118*, 9372.

(11) Hecker, W. C.; Bell, A. T. *J. Catal.* **1983**, *84*, 200.

(12) Oh, S. H.; Fisher, G. B.; Carpenter, J. E.; Wayne, D. *J. of Catal.* **1986**, *100*, 360. Oh, S. H.; Eickel, C. C. *J. Catal.* **1991**, *128*, 526.

(13) Cho, B. K. *J. Catal.* **1992**, *138*, 255; **1994**, *148*, 697.

(14) Permana, H.; Simon, K.; Peden, C.; Schmieg, S. J.; Belton, D. *J. Phys. Chem.* **1995**, *99*, 16344. Permana, H.; Simon, K.; Peden, C.; Schmieg, S. J.; Lambert, D. K.; Belton, D. *J. Catal.* **1996**, *164*, 194.

(15) Peden, C.; Belton, D.; Schmieg, S. J. *J. Catal.* **1995**, *155*, 204.

(16) Chuang S.; Tan, C. *J. Catal.* **1998**, *173*, 95.

(17) Granger, P.; Dathy, C.; Lecomte, J. J.; Leclercq, L.; Prigent, M.; Mabilon, G.; Leclercq, G. *J. Catal.* **1998**, *173*, 304. Granger, P.; Lecomte, J. J.; Dathy, C.; Leclercq, L.; Leclercq, G. *J. Catal.* **1998**, *175*, 194.

(18) Root, T. W.; Schmidt, L. D.; Fischer, G. B. *Surf. Sci.* **1983**, *134*, 30. Gopinath, Ch. S.; Zaera, F. *J. Catal.* **1999**, *186*, 387.

(19) McCabe, R. W.; Wong, Ch. *J. Catal.* **1990**, *121*, 422.

(20) Belton, D. N.; Schmieg, S. J. *J. Catal.* **1992**, *138*, 70.

(21) Sadhankar, R. R.; Ye, J.; Lynch, D. T. *J. Catal.* **1994**, *146*, 511. Sadhankar, R. R.; Lynch, D. T. *J. Catal.* **1994**, *149*, 278.

(22) Granger, P.; Malfoy, P.; Esteves, P.; Leclercq, L.; Leclercq, G. *J. Catal.* **1999**, *187*, 321.

(23) Granger, P.; Malfoy, P.; Leclercq, G. *J. Catal.* **2004**, *223*, 142.

(24) Cortes, J.; Araya, P.; Betancourt, F.; Diaz, F. *J. Chem. Res.* **2004**, *1*, 68−70.

(25) Belton, D. N.; DiMaggio, C. L.; Schmieg, S. J.; Ng, K. Y. S. *J. Catal.* **1995**, *157*, 559.

(26) Cortes, J.; Valencia, E. *Phys. Rev. B* **1994**, *49*, 16793. Cortes, J.; Valencia, E. *Phys. Rev. B* **1995**, *51*, 2621. Cortes, J.; Valencia, E. *Physica A* **2002**, *309*, 628. Valencia, E.; Cortes, J.; Puschmann, H. *Surf. Sci.* **2000**, *470*, L109. Cortes, J.; Valencia, E. *Phys. Rev. E* **2005**, *71*, 1.

(27) Cortes, J.; Valencia, E.; Araya, P. *J. Chem. Phys.* **1998**, *109*, 5607.

(28) Araya, P.; Porod, W.; Wolf, E. E. *Surf. Sci.* **1990**, *230*, 245. Araya, P.; Porod, W.; Snat, R.; Wolf, E. E. *Surf. Sci.* **1989**, *180*, 208.

(29) Olsson, L.; Zhdanov, V. P.; Kasemo, B. *Surf. Sci.* **2003**, *529*, 338.

(30) Stauffer, D.; Aharony, A. *Introduction to Percolation Theory*, 2nd ed.; Taylor and Francia: London, 1992.

(31) Hoshen, J.; Kopelman, R. *Phys. Rev. B* **1976**, *14*, 3438. Kopelman, R. *J. Stat. Phys.* **1986**, *42*, 185.